

# Static and Dynamic Calculation of Short-Circuit Currents in Synchronous Generators

T. A. Papadopoulos, Ch. G. Kaloudas, P. N. Papadopoulos, A. G. Marinopoulos, G. K. Papagiannis

**Abstract**— The calculation of short-circuit currents is mostly based on the methodology of the international standards IEC-60909 and ANSI/IEEE C37.010.1979. This methodology, although it utilizes simple procedures and various assumptions, usually provides satisfactory results. However, dynamic tools such as the ATP/EMTP can be used for the accurate simulation of short-circuit currents. In this paper the influence of some simplifying assumptions on the synchronous generator modeling in both standards is investigated and differences between the static and the dynamic analysis are examined, highlighting cases where significant discrepancies may occur. The analysis includes single or multiple generators connected to isolated or grid connected topologies.

**Keywords:** Short-circuit calculation, IEC 60909, ANSI, ATP/EMTP modeling.

## I. INTRODUCTION

THE calculation of the short circuit currents according to the IEC-60909 [1] and the ANSI [2] standards is one of the most common procedures for the power utility engineer. Both standards use a static calculation methodology, based on the equivalent voltage source method. This methodology can be used for the calculation of maximum and minimum SC currents, for both symmetrical and asymmetrical faults. However, more precise results can be derived by the calculation of SC currents from the actual waveforms that are obtained by the dynamic simulation of the fault conditions. The ATP/EMTP [3] software is a benchmark considering transient studies in power systems and is certainly capable of treating SC simulations [4].

In this paper, a thorough investigation of different SC scenarios in networks with synchronous generators is conducted. The methods of IEC-60909 and ANSI standards, as well as ATP/EMTP dynamic simulations have been used, since the combined calculations and the comparison of the results allow a better insight on the significance of all assumptions, used in the SC calculations and useful conclusions for practical engineering applications.

More specifically, the influence of the generator

subtransient performance on SC currents is examined for different SC conditions and network topologies of isolated and grid-connected generators. The effect of the fault location is also investigated and the analysis is extended to several topologies with synchronous generators. Results are evaluated using also the corresponding formulas for SC current calculations in synchronous generators [5].

## II. SYSTEM UNDER STUDY

The examined configuration is presented in Fig. 1 and consists of two synchronous generators and two step-up transformers connected through an Overhead Transmission Line (OHTL) to a busbar. The OHTL is of variable length  $\ell$  and its remote end ( $N_3$ ) is connected either to a local load, corresponding to an isolated network topology (Topology I), or to a stiff busbar, representing generators operating at a grid-connected topology (Topology II). In both cases generators are assumed to deliver rated power at nominal power factor for the steady-state condition preceding the fault. Generators and the wye side of the step-up transformers are directly grounded.

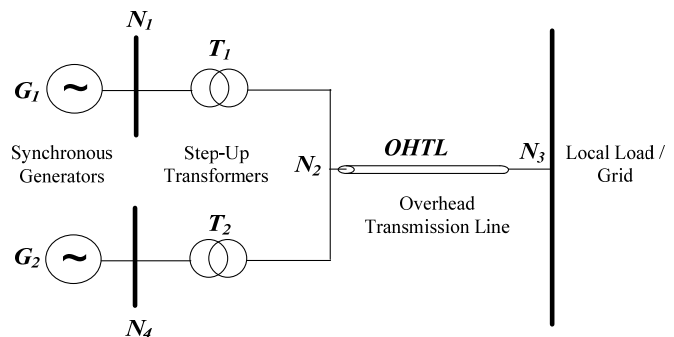


Fig. 1: System under study.

The above two network topologies are used to represent two different grid schemes characterized as  $G_S$  and  $G_L$ . In scheme  $G_S$ , two small hydro generators supply a 20 kV medium voltage distribution busbar, while in scheme  $G_L$ , two large gas turbine generators are connected to a 150 kV transmission busbar. The corresponding data are presented in Table I.

## III. SYSTEM MODELING

The Short-Circuit calculation process according to the IEC-60909 and ANSI standards is based on the equivalent voltage source method with certain assumptions. A thorough

T. A. Papadopoulos, Ch. G. Kaloudas, P. N. Papadopoulos and G. K. Papagiannis are with the Power Systems Laboratory, Department of Electrical and Computer Engineering, Aristotle University of Thessaloniki, Thessaloniki GR 54124, Greece (e-mail: grigoris@eng.auth.gr).

A. G. Marinopoulos is with ABB Corporate Research, Västerås, Sweden.

analysis on the two static approaches, considering the pre-fault conditions, the network topology representation and the SC current calculations have been presented in [4], [7] – [9]. On the other hand, ATP/EMTP offers an adequate simulation of the dynamic behavior of the whole system during the fault. For the dynamic simulation, generators, transformers and the OHTL are modeled using the Type 59 Synchronous Machine, the BCTRAN and the JMarti models, respectively [3], while the load is represented by an equivalent lumped R-L circuit.

TABLE I  
TEST CASE NETWORK DATA

Description	Symbol	Data	
		$G_L$	$G_S$
<b>Synchronous Generator</b>			
Rated Apparent Power (MVA)	$S_{G,r}$	161.7	1.35
Rated Voltage (kV)	$V_{G,r}$	15	0.6
Power Factor	$pf$	0.85 lagging	0.8 lagging
Synchronous Direct Axis Reactance (pu)	$X_d$	1.97	1.876
Transient Direct Axis Reactance (pu)	$X'_d$	0.22	0.211
Subtransient Direct Axis Reactance (pu)	$X''_d$	0.165	0.099
SC-Transient Time Constant (ms)	$T'_d$	940	346
SC-Subtransient Time Constant (ms)	$T''_d$	31	6
<b>Step-Up Transformer</b>			
Rated Apparent Power (MVA)	$S_{T,r}$	180	1.6
Rated Voltage (kV)	$V_{T1}/V_{T2}$	150/15	20/0.6
Impedance Voltage (pu)	$u_k$	0.152	0.061
Resistive Comp. of Impedance Voltage (pu)	$u_r$	0.002	0.0113
Vector Group	-	Yd5	Yd5
<b>Overhead Transmission Line</b>			
Positive Sequence OTL Impedance ( $\Omega/\text{km}$ )	$R'_1+jX'_1$	0.09+j0.42	0.3+j0.3
Zero Sequence OTL Impedance ( $\Omega/\text{km}$ )	$R'_0+jX'_0$	0.23+j1.31	0.5+j1.7

Although in SC analysis accurate frequency domain modeling of the network elements is not necessary, the JMarti model of ATP/EMTP has been selected in the analysis for the OHTL. This has been done in order to avoid possible conflicts from the combination of the lumped PI equivalent model capacitances and the lumped load impedance. However in both IEC 60909 and in the ANSI Standards simplified transmission line models are used, ignoring the shunt capacitances. Therefore in order to avoid errors due to the different line models, another simulation has been conducted using a R-L equivalent for the transmission line. SC current results are compared to the corresponding by the JMarti line model showing very good agreement.

Furthermore, in the dynamic simulation it is important to select the proper voltage conditions at the fault location, in order to calculate the highest SC current. The maximum peak and rms currents during a SC may occur at different times [10], thus two SC initialization times are examined. In the first

one the maximum peak current ( $i_{p-max}$ ) occurs, corresponding to the maximum dc offset when the voltage is zero, while at this case the initial symmetrical current is symbolized as  $I''_k @ i_{p-max}$ . In the second time the maximum initial symmetrical current is calculated ( $I''_{k-max}$ ) and the corresponding peak current is  $i_p @ I''_{k-max}$ . This is illustrated in Fig. 2a, where the three-phase SC current at  $N1$  is presented for different fault initialization times ( $t_{sc}$ ) and for the  $G_5$  generator in network Topology II, assuming only one generator in operation and the line length equal to 2 km. At  $t_{sc}$  equal to 16 ms  $i_{p-max}$  occurs, while at  $t_{sc}$  equal to 18 ms  $I''_{k-max}$  is recorded.

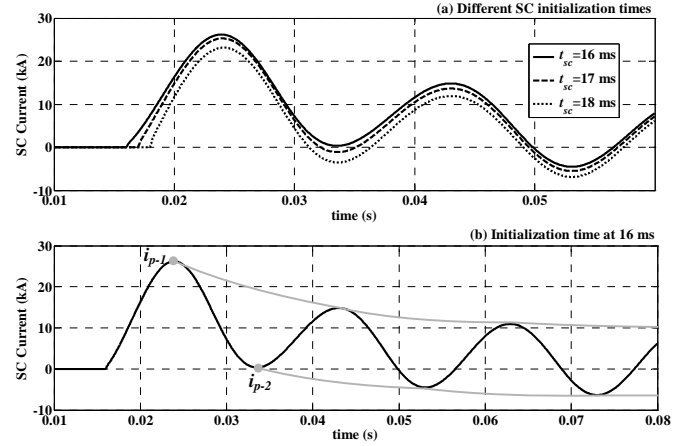


Fig. 2: Phase  $a$  current response during a three-phase SC at busbar  $N1$  for the interconnected small generator scheme (a) different SC initialization times (b) current envelopes for initialization time at 16 ms.

The initial symmetrical current in all cases is determined by the top and the bottom envelopes of the SC current [11]. Therefore,  $I''_k$  is computed using (1), as the sum or the difference of the two peak current values  $i_{p-1}$ ,  $i_{p-2}$  during the first SC current cycle.

$$I''_k = \frac{|i_{p-1}| \pm |i_{p-2}|}{2\sqrt{2}}, \quad (1)$$

The sum in the numerator corresponds to the case where there is a zero crossing between  $i_{p-1}$  and  $i_{p-2}$ , while the minus is used when both peak currents have the same sign.

#### IV. INFLUENCE OF GENERATORS SUBTRANSIENT PERFORMANCE

Both IEC-60909 and ANSI standards do not take into account the  $T''_d$  and  $T'_d$  time constants in SC calculations, which determine the subtransient and transient behavior of synchronous generators under fault conditions. In (A1) and (A3) of the Appendix the corresponding SC current formulas for the three- and single- phase to ground faults cases are presented, respectively, where the influence of  $T''_d$  and  $T'_d$  is shown analytically.

The influence of  $T''_d$  on SC currents is investigated, examining three- and single- phase to ground faults at busbar

$NI$ , using the ATP/EMTP software and the results are compared with the corresponding obtained by the IEC-60909 and ANSI standards. Both network schemes  $G_S$  and  $G_L$  as well as the two network topologies, for islanded network (Topology I) and for grid connected network (Topology II) are examined, assuming only generator  $G_I$  in operation and the line length equal to 2 km.

#### A. Three-phase to ground SC

SC currents calculated by the dynamic approach are shown in Table II. The percent differences between SC currents ( $I_{SC}$ ), obtained by the two static approaches and by the dynamic simulation, are calculated using (2). Differences for Topology I and Topology II networks are presented in Tables III and IV, respectively.

$$\text{difference}(\%) = 100 \cdot \left( 1 - \frac{I_{SC-\text{static procedure}}}{I_{SC-\text{dynamic simulation}}} \right), \quad (2)$$

where,  $I_{SC}$  can be  $i_{p-\max}$ ,  $I''_k @ i_{p-\max}$ ,  $i_p @ I''_{k-\max}$ ,  $I''_{k-\max}$ . Observing the results of Tables III and IV it must be noted that a minus sign means that the fault current results by the corresponding method are higher than the reference.

TABLE II

THREE-PHASE SC CURRENT AT BUSBAR  $NI$  CALCULATED BY ATP/EMTP

SC Current	SC time (ms)	Topology I (kA)	Topology II (kA)
<b>Large Generator</b>			
$i_{p-\max}$	15	108.0	113.84
$I''_k @ i_{p-\max}$	15	38.18	40.25
$i_p @ I''_{k-\max}$	15	108.0	113.84
$I''_{k-\max}$	15	38.18	40.25
<b>Small Generator</b>			
$i_{p-\max}$	16	25.321	26.195
$I''_k @ i_{p-\max}$	16	8.952	9.14
$i_p @ I''_{k-\max}$	18	22.601	23.134
$I''_{k-\max}$	18	9.153	9.427

TABLE III

% DIFFERENCES OF THREE-PHASE SC CURRENT AT BUSBAR  $NI$  FOR TOPOLOGY I

	ANSI	IEC max.	IEC min.
<b>Large Generator</b>			
$i_{p-\max}$	-24.44	-29.47	-
$I''_k @ i_{p-\max}$	-30.36	-38.95	-26.32
$i_p @ I''_{k-\max}$	-24.44	-29.47	-
$I''_{k-\max}$	-30.36	-38.95	-26.32
<b>Small Generator</b>			
$i_{p-\max}$	-38.33	-26.26	-9.04
$I''_k @ i_{p-\max}$	-44.91	-53.53	-32.59
$i_p @ I''_{k-\max}$	-54.98	-41.46	-22.17
$I''_{k-\max}$	-41.74	-50.15	-29.68

For the  $G_L$  scheme  $i_{p-\max}$  and  $I''_{k-\max}$  occur for faults occurring at 15 ms, while in  $G_S$  scheme the corresponding time is different, due to the lower value of  $T''_d$ . Next, comparing the results of the two network topologies, it is

shown that the differences in the results for the Topology II are 4 % to 6.5 % lower than the corresponding of Topology I. This is due to the different initial steady state conditions of the generator which are ignored in both standards [4], [7] – [9], while they are properly taken into account in ATP/EMTP.

For the  $G_S$  scheme per-cent differences may surpass 40 %, e.g. for  $I''_k @ i_{p-\max}$  current in Topology II. In the dynamic simulation  $I''_k$  is calculated using  $i_{p-1}$  and  $i_{p-2}$  of the top and bottom envelopes, as shown in Fig. 2b [1]. Current  $i_{p-1}$  is 26.19 kA, while  $i_{p-2}$  is 0.34 kA, thus  $I''_k$  is 9.14 kA. The initial symmetrical current values calculated with the IEC and the ANSI Std. are 13.744 kA and 12.973 kA, respectively, and the corresponding differences are -41.91 % and -50.37 %, given in Table IV.

Comparing the two generator schemes it is observed that for the  $G_S$  scheme, in general, SC currents calculated by the dynamic simulation show higher deviation from the corresponding SC currents of the two standards, while these differences for  $G_L$  topology are significantly lower.

This is attributed to the value of  $T''_d$ , which is taken into account in dynamic simulation, allowing the exact recording of the subtransient performance of the generator. As shown in Table I, the value of  $T''_d$  for the large generator is higher compared to the corresponding of the small generator.

TABLE IV

% DIFFERENCES OF THREE-PHASE SC CURRENT AT NODE  $NI$  FOR TOPOLOGY II

	ANSI	IEC max.	IEC min.
<b>Large Generator</b>			
$i_{p-\max}$	-18.06	-22.82	-
$I''_k @ i_{p-\max}$	-23.68	-31.82	-19.84
$i_p @ I''_{k-\max}$	-18.06	-22.82	-
$I''_{k-\max}$	-23.68	-31.82	-19.84
<b>Small Generator</b>			
$i_{p-\max}$	-33.72	-22.05	-
$I''_k @ i_{p-\max}$	-41.91	-50.37	-29.87
$i_p @ I''_{k-\max}$	-51.41	-38.20	-
$I''_{k-\max}$	-37.62	-45.79	-25.91

Both  $I''_k$  and  $i_p$  are influenced by the subtransient performance of the generator which takes place within the very first milliseconds of the fault. Therefore, higher  $T''_d$  values result in longer subtransient times, which is a condition more close to the methodology of calculation of  $I''_k$  and  $i_p$  SC currents in IEC and ANSI standards. This is also illustrated in Fig. 3, where  $\exp(-t/T''_d)$ , defined in (A2b) assuming  $X_e$  equal to zero, is plotted for the  $G_L$  and  $G_S$  topologies, while  $T''_d$  takes different values. As  $T''_d$  increases, the term  $\exp(-t/T''_d)$  acquires higher values, resulting in longer subtransient periods, as occurs from (A1).

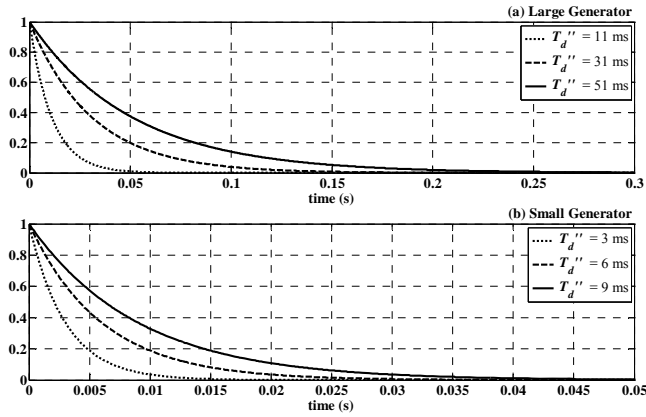


Fig. 3: Values of  $\exp(-t/T_d'')$  term vs time for the (a) Large and (b) Small generators.

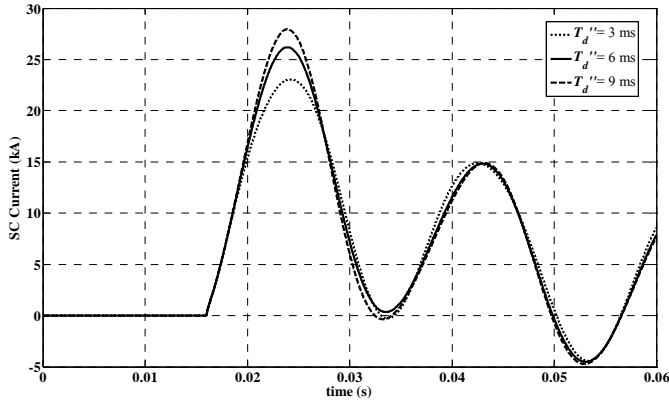


Fig. 4: Phase  $a$  current responses during a three-phase SC at busbar  $NI$  for the interconnected small generator scheme and different  $T_d''$  values. SC at 16 ms.

Current responses at busbar  $NI$  for the different values of  $T_d''$  and network scheme  $G_S$  operating in interconnected mode is presented in Fig. 4. The SC occurs at 16 ms, i.e. the case where the maximum peak current is recorded. As  $T_d''$  increases the first cycle peak current acquires higher values and the differences between the dynamic simulation results and the corresponding IEC SC currents are gradually reduced. The per cent differences of  $I''_k$  and  $i_p$  compared to the corresponding maximum values of the IEC are -37.32 % and -14.39 %, respectively.

The obtained results show that practically both IEC and ANSI standards treat synchronous generators with large  $T_d''$  in SC calculations more accurately than generators with small short circuit time constants.

### B. Single-phase to ground SC

Single-phase to ground SC current calculations are presented in Table V for the scheme  $G_S$  in Topology II. In this test case SC currents  $i_{p-max}$  and  $I''_{k-max}$  occur both for faults starting at 15 ms.

The corresponding differences of the SC currents acquire significantly lower values compared to the corresponding results of Table IV for the three-phase to ground fault. This is again attributed to the different value of  $T_d''$  for the single-phase to ground fault, defined in (A4c).

TABLE V  
% DIFFERENCES OF SINGLE-PHASE TO GROUND SC CURRENT AT BUSBAR  $NI$  FOR THE SMALL GENERATOR TOPOLOGY

	ANSI	IEC max.	IEC min.	ATP/EMTP
<b>Large Generator</b>				
$i_p$	-10.27	-14.72	-	134.42 kA
$I''_k$	-14.57	-22.11	-11.00	47.92 kA
<b>Small Generator</b>				
$i_p$	-19.18	-8.78	-	33.21 kA
$I''_k$	-1.47	-7.50	7.16	14.45 kA

In Table VI it is shown that the subtransient and transient time constants of the small generator for the single-phase to ground fault are higher than the corresponding for the three-phase to ground case, thus resulting in fault currents which are closer to those calculated by the IEC and ANSI approaches.

TABLE VI  
TIME CONSTANTS OF THE SMALL GENERATOR FOR THE THREE- AND SINGLE-PHASE TO GROUND SC

Time Constant	Three-Phase	Single-Phase
$T_d$ (ms)	21	19
$T_d'$ (ms)	346	564
$T_d''$ (ms)	6	9

## V. INFLUENCE OF THE FAULT LOCATION

The effect of the electrical distance between the generator and the SC fault location is investigated. The  $G_S$  Topology II scheme with only  $G_I$  generator in operation is considered, while the fault location is assumed at busbars  $NI$ ,  $N2$  and  $N3$  of the network in Fig. 1.

The per cent differences of SC currents for the IEC 60909 and ANSI standards are presented in Table VII for three- and single- phase to ground faults. At the dynamic simulation the maximum values of SC currents  $i_p$  and  $I''_k$  occurred at different times, thus the corresponding values are presented in the grey outlined rows of the same table.

TABLE VII  
% DIFFERENCES OF THREE- AND SINGLE- PHASE TO GROUND SC CURRENTS FOR  $G_S$ - TOPOLOGY II

Fault Position	$NI$		$N2$		$N3$	
	3-ph	1-ph	3-ph	1-ph	3-ph	1-ph
Fault Type	3-ph	1-ph	3-ph	1-ph	3-ph	1-ph
	<b><math>i_p</math> SC current</b>					
ANSI exact	-14.4	-0.21	-4.59	3.62	-3.15	5.91
ANSI 2.7 factor	-33.72	-19.18	-23.93	-14.49	-23.73	-13.56
IEC	-22.05	-8.77	-11.43	-2.98	-9.94	-1.07
ATP /EMTP (kA)	26.20	33.21	0.560	0.774	0.552	0.744
<b><math>I''_k</math> SC current</b>						
ANSI	-37.62	-1.47	-15.77	3.81	-15.00	5.15
IEC max.	-45.79	-7.49	-22.52	-1.76	-21.81	-0.61
IEC min.	-25.91	7.16	-11.71	7.33	-10.91	8.48
ATP /EMTP (kA)	9.427	14.45	0.222	0.341	0.220	0.330

Considering the SC calculations with the ANSI Std.,  $i_p$  current is calculated using the coefficient derived by the actual  $X/R$  as well as by the approximate coefficient 2.7 [2]. The exact approach results in all cases to lower differences than with the approximate approach. Differences between the ANSI Std. and the dynamic simulation for the single-phase to ground case are practically negligible and have lower values than the minimum IEC SC currents in most cases, as shown in Table VII.

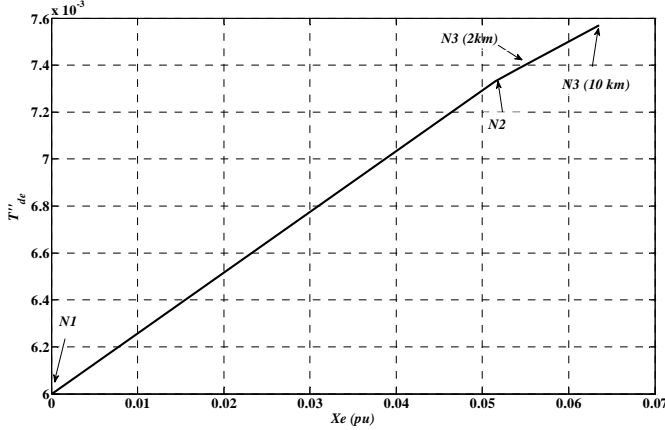


Fig. 5: Three-phase equivalent subtransient time constant  $T''_{de}$  against variable external impedance.

Absolute differences between the two static approaches and the dynamic simulation are gradually decreased as the fault location distance from the generator increases for both three- and single- phase faults. This is due to the fact that the equivalent subtransient time constant  $T''_{de}$  is an increasing function with fault distance as shown in Fig. 5, where (A2b) is plotted against different values of the external impedance  $X_e$ , thus resulting in longer subtransient performance periods. The line length is assumed to be variable with length 2 and 10 km.

For the three-phase to ground fault, SC current results by the ATP/EMTP simulation are in all cases lower than the corresponding minimum SC currents of the IEC, while for the single phase to ground fault, the dynamic simulation results are between the minimum and the maximum  $I''_k$  and  $i_p$  currents, according to IEC. Differences between the two static approaches and the dynamic simulation are more severe for the three-phase to ground fault than for the single-phase to ground case.

## VI. MULTIPLE GENERATOR ARRANGEMENT

In this section the case of multiply fed short-circuits is investigated, using the generalized network arrangement of Fig. 1, where both generators are connected to the network. Schemes  $G_L$  and  $G_S$  are examined connected in Topology II and the corresponding differences between the SC obtained by the static approaches and the dynamic simulation are presented in Tables VIII and IX, respectively. SC currents  $i_p$  and  $I''_k$  correspond to the maximum value recorded at the corresponding time interval.

TABLE VIII  
% DIFFERENCES OF THREE- AND SINGLE- PHASE TO GROUND SC CURRENTS  
FOR TWO  $G_L$  GENERATORS – TOPOLOGY II

Fault Position	N1/N4		N2		N3	
	3-ph	1-ph	3-ph	1-ph	3-ph	1-ph
<b><math>i_p</math> SC current</b>						
ANSI exact	9.46	1.55	12.92	3.80	13.56	4.93
ANSI 2.7 factor	11.44	5.73	14.92	4.35	14.65	6.15
IEC	4.36	-3.69	5.46	-5.21	6.09	-3.91
ATP /EMTP (kA)	158.3	171.6	13.09	15.96	12.55	14.63
<b><math>I''_k</math> SC current</b>						
ANSI	7.76	4.94	12.81	5.54	13.29	6.64
IEC max.	-1.21	-4.00	2.87	-5.93	3.45	-4.49
IEC min.	7.99	5.45	11.71	3.70	12.24	5.02
ATP /EMTP (kA)	56.28	64.38	4.73	5.89	4.57	5.45

Fault locations of three- and single- phase to ground short circuits are assumed at the busbars  $N1 - N4$ . SC currents recorded at the faulted busbars  $N1$  and  $N4$  gave identical results, due to the network electrical symmetry, thus the corresponding results are noted as  $N1/N4$ . In such complex network topologies it is difficult to analyze and calculate the SC currents, using analytical formulas or an equivalent circuit with a single equivalent time constant, as in the previous topologies [5].

First, comparing the corresponding ANSI SC currents it is shown that for the  $G_L$  generator scheme, the ANSI approach significantly underestimates the SC currents and especially  $i_p$  when calculated with the approximate coefficient 2.7. The exact  $X/R$  ratio takes values from 43.5 to 62.5, depending on the fault location and so is significantly higher than that assumed for the 2.7 coefficient approximation calculation [2]. For the  $G_S$  scheme, the ANSI approach significantly over-estimates the three-phase SC currents.

Results of the IEC  $i_p$  and the maximum  $I''_k$  SC currents for the three-phase to ground fault for the  $G_L$  scheme are slightly underestimated than the corresponding dynamic simulation results, especially as the faulted node is electrically located further from the two generators. On the contrary for the  $G_S$  scheme, where the  $X/R$  ratio is significantly lower and takes values from 5.3 to 6.1, the IEC method strongly overestimates the corresponding three-phase to ground SC currents.

For both network schemes  $I''_k$  single-phase to ground SC currents calculated by the ATP/EMTP are between the corresponding maximum and minimum limits defined by the IEC Std. In general the degree of the over- and underestimation of the two static approaches varies with initial magnitude of each SC current source and the corresponding time constants [5] and therefore further systematic analysis is needed.

TABLE IX  
% DIFFERENCES OF THREE- AND SINGLE- PHASE TO GROUND SC CURRENTS  
FOR TWO  $G_s$  GENERATORS – TOPOLOGY II

Fault Position	N1/N4		N2		N3	
	3-ph	1-ph	3-ph	1-ph	3-ph	1-ph
$i_p$ SC current						
ANSI exact	-8.59	1.077	-4.50	3.61	-1.82	7.12
ANSI 2.7 factor	-31.81	-20.06	-23.82	-14.12	-23.71	-12.74
IEC	-19.82	-2.76	-11.42	-1.61	-8.73	0.77
ATP /EMTP (kA)	39.68	44.067	1.121	1.551	1.088	1.437
$I''_k$ SC current						
ANSI	-27.83	3.21	-16.03	4.09	-14.22	6.69
IEC max.	-35.85	-2.76	-23.02	-1.61	-21.33	0.78
IEC min.	-17.32	11.25	-11.74	7.60	-9.86	10.26
ATP /EMTP (kA)	15.15	20.25	0.443	0.684	0.436	0.643

## VII. CONCLUSIONS

In this work different symmetrical three- and unsymmetrical single- phase to ground SC scenarios involving synchronous generators operating either in an isolated network or in a grid-connected topology have been investigated. Results obtained by the widely used ANSI and IEC 60909 standards and by dynamic simulation using the ATP/EMTP software are compared in order to evaluate the influence of various parameters.

For the case of the grid-connected generator the short-circuit currents calculated by the two static approaches of the Standards are closer to those obtained by the dynamic simulation, compared to the corresponding results for the isolated network topology. Therefore, in isolated networks, as in the islanded mode of operation, significant errors may occur in the calculation of SC currents calculated by IEC-60909 and ANSI/IEEE, in cases where generators are present.

It is shown that the influence of the generator subtransient time constant on the fault current magnitude is significant. This parameter strongly affects the initial fault current response. In both IEC 60909 and ANSI standards it is neglected, thus resulting in significant differences in the SC current calculations especially for cases where synchronous generators are characterized by very short subtransient time constants. Similarly the influence of the fault location is examined. It is shown that as the electrical distance between the fault point and the generator increases, differences between the two static approaches and the dynamic simulation are gradually reduced, since the equivalent subtransient time constant of the network increases, thus resulting in lower subtransient periods.

The investigation is extended for multiply fed faults, examining the simultaneous operation of two synchronous

generators. Overestimated and underestimated currents by the two static approaches are recorded, depending on various parameters and therefore general conclusion cannot be derived and further systematic analysis is necessary.

The calculation procedures described in both IEC 60909 and ANSI standards, are generally accepted as efficient methods, leading to results that in most cases rely on the safe side. However, there are certain cases, especially at the presence of multiple generators, where the user must be quite careful to avoid overestimation or, even worse, underestimation of the protection equipment. This paper provides a better insight in the calculation of fault currents by IEC, ANSI and dynamic simulation, highlighting cases where such discrepancies may occur.

## VIII. APPENDIX

In the generalized case where a three-phase SC occurs at a distant fault location from the generator terminals through an external equivalent impedance  $X_e$ , the peak current envelope at any time instant is given by (A1) [5].

$$\hat{i}_r(t) = \sqrt{2}E_0 \left[ \frac{1}{X_d + X_e} + \left( \frac{1}{X'_d + X_e} - \frac{1}{X_d + X_e} \right) e^{-t/T'_{de}} \right] + \left( \frac{1}{X''_d + X_e} - \frac{1}{X'_d + X_e} \right) e^{-t/T''_{de}} + \frac{1}{X''_d + X_e} e^{-t/T_a} \quad (A1)$$

where:

$$T'_{de} = \frac{X'_d + X_e}{X_d + X_e} \times \frac{X_d}{X'_d} T'_d \quad (A2a)$$

$$T''_{de} = \frac{X''_d + X_e}{X'_d + X_e} \times \frac{X'_d}{X''_d} T''_d \quad (A2b)$$

$$T_a = \frac{X''_d}{\omega_s R_a} \quad (A2c)$$

and  $R_a$  is the stator dc resistance.

The corresponding equation for an unbalanced single-phase to ground SC at the poles of the generator is [5]:

$$\hat{i}_r(t) = 3\sqrt{2}E_0 \left[ \frac{1}{X_d + X_e^{NZ}} + \left( \frac{1}{X'_d + X_e^{NZ}} - \frac{1}{X_d + X_e^{NZ}} \right) e^{-t/T'_{d(1\phi)}} \right] + \left( \frac{1}{X''_d + X_e^{NZ}} - \frac{1}{X'_d + X_e^{NZ}} \right) e^{-t/T''_{d(1\phi)}} + \frac{1}{X''_d + X_e^{NZ}} e^{-t/T_{a(1\phi)}} \quad (A3)$$

where:

$$X^{NZ} = X^N + X^Z \quad (A4a)$$

$$T'_{d(1\phi)} = \frac{X'_d + X^{NZ}}{X_d + X^{NZ}} T'_{do} \quad (A4b)$$

$$T''_{d(1\phi)} = \frac{X''_d + X^{NZ}}{X'_d + X^{NZ}} T''_{do} \quad (A4c)$$

$$T_{a(1\phi)} = \frac{X''_d + X^{NZ}}{\omega_s R_a} \quad (A4d)$$

and  $X^N$ ,  $X^Z$  are the generator negative and zero sequence

impedances, respectively.

#### IX. REFERENCES

- [1] *Short-Circuit Currents in Three-Phase AC Systems*, IEC Standard 60909. part 0 and 1, 1<sup>st</sup> edition, 2001-7.
- [2] ANSI/IEEE Std 141, "*IEEE Recommended practice for Electric Power Distribution for Industrial plants*", Red Book, 1986.
- [3] H.W. Dommel, *EMTP Theory Book*. Bonneville Power Administration, Portland, OR, 1986.
- [4] A. Berizzi, S. Massucco, A. Silvestri, "Short-Circuit Current Calculation: A Comparison between Methods of IEC and ANSI Standards Using Dynamic Simulation as Reference", *IEEE Trans. on Industry Applications*, Vol. 30, No 4., July/August 1994. Pp. 1099-1106.
- [5] N. Tleis, *Power Systems Modeling and Fault Analysis*, Elsevier Ltd, 2008.
- [6] C. N. Hartman, "Understanding asymmetry," *IEEE Trans. Industry Applications*, vol. IA-21, no. 4, pp. 267-273, July/Aug. 1985.
- [7] G. Knight, H. Sieling, "*Comparison of ANSI and IEC 909 Short-Circuit Current Calculation Procedures*", *IEEE Trans. on Industry Applications*, Vol. 29, no. 3, May/June 1993, pp. 625-630.
- [8] Ch. G. Kaloudas, P. N. Papadopoulos, T. A. Papadopoulos, A. G. Marinopoulos, G. K. Papagiannis, "Short-Circuit Analysis of an Isolated Generator and Comparative Study of IEC, ANSI and Dynamic Simulation," presented at the MedPower 10 Conf., Agia Napa, Cyprus, 2010.
- [9] A. J. Rodolakis, "*A comparison of North American (ANSI) and European (IEC) Fault Calculation Guidelines*", *Industry Applications Society Annual Meeting*, Dearborn U.S.A., 1991.
- [10] H. W. Reichenstein, J. C. Gomez, "Relationship of  $X/R$ ,  $I_p$  and  $I_{rms}$  to Asymmetry in Resistance/Reactance Circuits," *IEEE Trans. Industry Applications*, vol. IA-21, no. 4, pp. 267-273, July/Aug. 1985.
- [11] F. Castelli, A. Silvestri, D. Zaninelli, "The IEC 909 Standard and Dynamic Simulation of Short-Circuit Currents", *ETEP*, Vol. 4, No 3, May/June 1994. Pp. 213-221.